Probing the Interdigitated Phase of a DPPC Lipid Bilayer by Micropipette Aspiration

*Hung V. Ly, Marjorie L. Longo**

Department of Chemical Engineering and Material Science, University of California, Davis, CA 95616, USA
E-mail: mllongo@ucdavis.edu

Summary: We used micropipette aspiration of giant unilamellar vesicles to directly measure the areal expansion of gel ($L_{\beta'}$) phase 1,2-dipalmitoyl-sn-glycero-3-phosphocholine (DPPC) lipid bilayers induced by exposure to ethanol/water mixtures. Areal expansion began in 7 vol% ethanol and increased monotonically as the concentration of ethanol was increased to 15 vol% at which point areal expansion reached a plateau of 50%. This ethanol concentration range is in good agreement with that of the interdigitated phase ($L_{\beta}I$) of DPPC, therefore, we believe that this is the first direct measurement of the areal expansion accompanying interdigitation of gel-phase lipids. Our observations are consistent with the presence of coexisting $L_{\beta}I$ and $L_{\beta'}$ phases in ethanol concentrations between 7% and 15 vol% and 100% $L_{\beta}I$ phase in 15 vol% ethanol and higher. We observed a bimodal distribution of areal expansion (0% and 20%) induced by 7 vol% ethanol indicating that at the threshold concentration, interdigitation is induced in only a portion of DPPC vesicles. Areal expansion could not be easily reversed, consistent with kinetic trapping of the $L_{\beta}I$ phase. DPPC vesicles exposed to butanol at the known threshold and plateau concentrations for the $L_{\beta}I$ phase displayed areal expansion behavior consistent with our ethanol observations. However, the area expanded significantly faster for DPPC bilayers exposed to butanol vs. ethanol, which we attribute to enhanced partitioning of the longer-chained butanol into the lipid headgroups. Ethanol-induced areal expansion of DPPC bilayers was inhibited by inclusion of 10 mol% and 25 mol% cholesterol in the bilayer. However, areal expansion could be induced by application of tensions (~8 mN/m) similar to the phenomena of interdigitation induced by high pressure. The presence of 20 vol% ethanol significantly decreased surface cohesion of DPPC bilayers containing 25 mol% cholesterol as evidenced by a decreased area compressibility modulus and lysis tension.

Keywords: area compressibility modulus; cholesterol, DPPC; ethanol; phase separation; rupture tension; Traube's rule

Introduction

Phosphatidylcholine (PC) lipids can exist in a phase in which the acyl chains from the opposing halves of the bilayer are fully interdigitated.[1] A transition from the gel-phase ($L_{\beta'}$) to the interdigitated phase ($L_{\beta}I$) is induced by the addition of short-chain alcohols or

 DOI: 10.1002/masy.200550110

other small molecules (ethylene glycol, Tris, anesthetics, etc.) to the surrounding aqueous media, or high hydrostatic pressure.[2] The physical structure and thermodynamic properties of the $L_{\beta}I$ phase have been well characterized by many techniques, including X-ray diffraction,[1] neutron diffraction,[3] fluorescence probes,[4] and differential scanning calorimetry (DSC).[5] Many of these studies were aimed at determining the degree of membrane thinning and phase transition temperature as well as the threshold concentrations and pressure of the $L_{\beta'}$-$L_{\beta}I$ phase transition. The mechanism behind the induction of the $L_{\beta}I$ phase has been attributed to the binding of the short-chain alcohols to the phospholipid bilayers in the $L_{\beta'}$ phase. The presence of the alcohols in the headgroup region increases the lateral and transverse repulsion between the lipid molecules that is first relieved by the tilting of the hydrocarbon chain and followed by chain interdigitation.[6,7] Biologically, the substantial thickness changes that accompany $L_{\beta'}$-$L_{\beta}I$ transition (e.g. 33%) should strongly affect the normal functions of membrane-associated proteins due to the mismatch of the hydrophobic region. Therefore, the role of the $L_{\beta}I$ phase in alcohol toxicity, alcohol tolerance, general anesthesia, cell viability, food sterilization, membrane fusion, and metabolic changes is of great interest.[8-10] In addition, the $L_{\beta'}$-$L_{\beta}I$ phase transition has been utilized in the formation of drug delivery vehicles.[11] It has also been found that the transition can be inhibited by the addition of cholesterol (Chol) in PC bilayers where the cholesterol alleviates the lipid head-group crowding that favors interdigitation.[12,13]

Inspired by our previous work where we demonstrated that short-chain alcohols (methanol, ethanol, propanol, and butanol) can significantly modify the mechanical properties and increase the area per molecule of fluid-phase PCs,[14] we now explore the $L_{\beta'}$-$L_{\beta}I$ phase transition and $L_{\beta}I$ phase of gel-phase PCs by micropipette aspiration (MPA). For a general review and the theoretical framework of the technique, see Needham and Zhelev.[15,16] Unlike other techniques (e.g. X-ray diffraction or neutron diffraction) that average over a large population of multilamellar vesicles, the MPA technique provides a unique opportunity to probe directly the structural and mechanical properties of the single bilayer of individual giant vesicles from 20 to 40 μm in diameter. MPA has been applied successfully to measure the mechanical and viscous properties of natural and synthetic systems (i.e. red blood cells,[17] egg lecithin vesicle,[18] and diblock polymers[19]) and the adsorption of small molecules into the bilayer and the accompanying area expansion (e.g.

the influenza hemagglutinin fusion peptide[20-22] and lysolipid[23]). Using MPA on giant unilamellar DPPC vesicles, we observe substantial area expansion (20-80%) of DPPC membranes undergoing the $L_{\beta'}$-$L_{\beta}I$ phase transition when exposed to ethanol-water or butanol-water mixtures and subsequent kinetic trapping of the $L_{\beta}I$ phase. We find that the $L_{\beta'}$-$L_{\beta}I$ phase transition is not induced in all vesicles at the threshold concentration of alcohol. In addition, the rate of membrane area expansion is substantially faster for exposure to butanol than exposure to ethanol. We explore the inhibiting effect of cholesterol (10 and 25 mol%) and show that it is possible for ethanol to decrease the mechanical cohesion of DPPC membranes containing cholesterol. It is shown that the inhibitory effect of cholesterol can be overcome by application of membrane tension. Also discussed are morphologies of DPPC vesicles in aqueous and ethanol-water environments and the lysis tensions and area compressibility moduli of DPPC, DPPC/10 mol% Chol, and DPPC/25 mol% Chol.

Experimental Section

Materials

1,2-dipalmitoyl-sn-glycero-3-phosphocholine and cholesterol in chloroform were purchased and used without further purification from Avanti Polar Lipids (Alabaster, AL). Ethanol (200 Proof) was bought from Gold Shield Chemical Co. (Hayward, CA). 1-butanol, sucrose, and glucose of high grade were bought from Sigma-Aldrich (St. Louis, MO). Chloroform and methanol were purchased from Fisher Scientific (Fairlawn, NJ). Bovine serum albumin (fraction V, low heavy metals) was purchased from Calbiochem (San Diego, CA). Deionized water used was produced by a Barnstead nanopure water system (Dubuque, IA) and had a resistivity of 18.1 MΩ-cm.

Giant Vesicles Preparation

We formed giant unilamellar vesicles composed of DPPC and Chol by the electroformation technique.[24] Briefly, stock solutions of DPPC and Chol were both diluted to 0.5 mg/ml solution in chloroform/methanol (2:1 volume ratio). Appropriate amounts of DPPC and Chol were premixed to have solutions with 9:1 and 3:1 (mol:mol) DPPC:Chol. We spread 50 μl of the premixed solution onto two platinum wires housed in an open Telfon® block that was then placed under vacuum for over 2 hours to remove any

trace amount of solvent. We sealed the open volume around the wires in the block with coverslips coated with SurfaSil® (Pierce, Rockford, IL). We next filled the volume with 100 mM sucrose aqueous solution (the vesicle's interior solution) that was preheated to ~50°C, above DPPC's phase transition temperature of 41°C.[25] Afterward, we submerged the block in a glass bowl filled with 100 mM sucrose aqueous solution, preheated to ~50°C. With the glass bowl in an oven set at ~50°C, we applied a 3 volt sine wave across the two wires at decreasing frequency loads (10 Hz for 30 min, 3 Hz for 15 min, 1 Hz for 7 min, and 0.5 Hz for 7 min). As noted by other investigators, giant vesicles formed best above its phase transition temperature.[26] Giant vesicles from 10 to 50 μm in diameters formed on the electrodes, and we cooled the vesicles to room temperature (~23 °C) at a cooling rate of ~0.28 °C/min. We harvested the vesicles in eppendorf vials and used them within a few days.

Micropipette Aspiration

Vesicles in an aqueous media were viewed with an inverted Nikon Diaphot 300 microscope (Nikon INC, Melville, NY) equipped with a 40X Hoffman modulation contrast objective (Modulation Optics, Greenvale, NY). The aqueous media containing the immersed 100 mM sucrose-filled vesicles varied from either 85 or 100 mM glucose with or without alcohol, depending on the type of experiments. Morphologies of DPPC vesicles were viewed in isotonic 100 mM glucose solutions. Flow-pipette MPA experiments on DPPC vesicles were performed in exterior 85 mM glucose solutions while flow-pipette MPA, area compressibility, and lysis tension experiments on DPPC/Chol vesicles were conducted in exterior 100 mM glucose solutions. The micropipettes used for holding vesicles were filled with a 100 mM glucose, 0.02 wt% albumin solution, and the tips of the micropipettes were coated with SurfaSil®. Micromanipulation of the vesicles and other details of the micropipette aspiration setup were thoroughly discussed in our previous paper,[14] and we note only changes in procedure here.

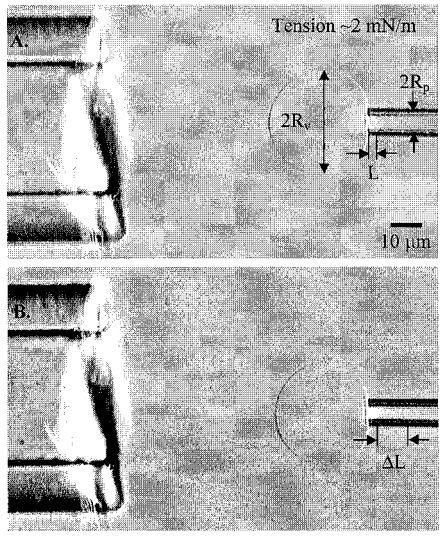

Figure 1 Microscope images of a weakly aspirated giant DPPC vesicle inside a micropipette. A flow pipette delivering a stream of an isotonic glucose media with 10 vol% ethanol is placed in front of the vesicle. **(A)** The initial length of the projection, L, before the flow is activated. **(B)** The projection length grew, ΔL, as the membrane underwent the $L_{\beta'}$-$L_{\beta}I$ phase transition. ΔL is proportional to the membrane area expansion, $(\Delta A/A_{0\%})_{exp}$.

We applied the micropipette aspiration technique developed by Evans and co-workers[18] to measure three mechanical properties of DPPC/Chol vesicles exposed to an alcohol/water mixture: membrane area expansion, area compressibility modulus, and lysis tension. We measured the area expansion by first weakly aspirating individual vesicles into a micropipette (7-9 μm in diameter). The aspirated vesicles (enclosing 100 mM sucrose) were suspended in an outside 85 mM glucose mixture where the difference in osmolarity swelled the vesicles into almost spherical shapes. Seleçted vesicles appeared clear (no trapped internal smaller vesicles), unilamellar, and ranged in size from 20 to 40 μm in diameter. Each aspirated vesicle was then prestretched beyond 7 mN/m for 1-2 seconds and relaxed back to a holding tension of ~2 mN/m. We next placed a flow pipette (100-150 μm in diameter) directly in front of the aspirated vesicle (see figure 1) to deliver a constant flow of an isotonic 85 mM glucose, alcohol/water mixture around the vesicle. The flow was driven by a syringe pump (KD Scientific Model 200, New Hope, PA) for constant velocities between 100 to 200 μm/s. The alcohol's interaction with the vesicle

caused the vesicle's projection, L, inside the micropipette to elongate dramatically (see figure 1B) and for the spherical portion of the vesicle outside the micropipette to shrink in diameter. We video recorded this dynamic growth, ΔL, of the projection length and the decrease in the outer vesicle's radius until the projection length reached a plateau or the vesicle collapsed inside the micropipette. Collapse occurred quickly within 1-2 seconds. We subsequently analyzed the tapes to convert these vesicle's geometric parameters into an apparent area expansion, $(\Delta A/A_{0\%})_{exp}=(A-A_{0\%})/A_{0\%}$ with the following equation with the inherent assumption that the volume of the aspirated vesicle remained constant.[27]

$$\left(\frac{\Delta A}{A_{0\%}}\right)_{exp} = \frac{2\pi R_p \Delta L}{A_{0\%}}\left(1-\frac{R_p}{R_v}\right) \quad (1)$$

We approximated the oblate shape of the aspirated vesicle as a sphere with an averaged radius, R_v. $A_{0\%}$ is the measured surface area of the vesicle before alcohol exposure, A is the surface area after exposure, and R_p is the radius of the micropipette. We confirmed that for vesicles exposed to a high ethanol concentration of 10 vol%, the volume of the individual aspirated vesicle (from measuring the projection growth, ΔL, and decreases in R_v) as a function of time until the projection reached a stable plateau was conserved. The differences in these measured time-elapsed volumes was less than or fell within the individual measured volume's uncertainty of 7%-14% for vesicles ranging from 20 to 40 μm in diameters with an optical resolution limitation of 0.5 to 1 μm.

The area compressibility modulus, K_{app}, represents the resistance to fractional membrane area dilation, $\alpha=(A-A_o)/A_o$, from an applied isotropic tension, τ, where A_o is the membrane area of the vesicle measured at an initial low tension state. We determined K_{app} for each giant DPPC/Chol vesicle by first weakly aspirating it inside a micropipette. Each vesicle was prestressed beyond 7 mN/m for 1-2 seconds to smooth out any folds or tethers in the membrane and relaxed back to a desired low tension of ~1 mN/m. The applied suction pressure, ΔP, holding the vesicle was next increased in a stepwise manner to induce an incremental deformation change, ΔL, in the vesicle's projection, L, inside the micropipette. For each pressure change, ΔP was held constant for at least five seconds to ensure that L has reached equilibrium. We recorded these stress-strain measurements onto videotapes and later analyzed the vesicle images to measure α and τ. α was calculated with equation 1 whereas τ was computed from approximating the oblate shape of the vesicle as a sphere with an averaged radius, R_v:[27]

$$\tau = \frac{\Delta P \, R_p}{2\left(1 - \frac{R_p}{R_v}\right)} \tag{2}$$

The plot of τ versus α exhibited a linear relationship, and the slope of this line by convention is known as the apparent area compressibility modulus, K_{app}, i.e. $\tau = K_{app}\alpha$.[28] Lysis tension, τ_{lys}, is the highest mechanical tension the vesicle can sustain before rupturing or collapsing. We measured τ_{lys} of DPPC vesicles in 100 mM glucose at a pulling rate of 0.1 mN/m/s and in 85 mM glucose at a pulling rate of 0.5 mN/m/s. DPPC/Chol vesicles were measured in 100 mM glucose mixtures with and without alcohol at pulling rates of 0.2 mN/m/s and 0.7 mN/m/s respectively.

Results and Discussion

Surface Morphology and Membrane Failure of DPPC Vesicles

A major experimental objective of this work was to subject giant DPPC vesicles to flows of ethanol solutions while being held by micropipette aspiration. The subsequent increases in membrane projection lengths would allow us to quantify membrane area expansion $(\Delta A/A_{0\%})_{exp}$ accompanying the $L_{\beta'}$-$L_{\beta}I$ phase transition. However, in order to successfully carry out this experiment, aspirated DPPC vesicles must have a smooth surface so that $(\Delta A/A_{0\%})_{exp}$ represents the $L_{\beta'}$-$L_{\beta}I$ phase transition rather than smoothing of sharp membrane contours, aspirated vesicles must be robust enough to stay intact under an applied tension, and DPPC vesicles must still remain as stable vesicles after the $L_{\beta'}$-$L_{\beta}I$ phase transition. Therefore, we characterized giant DPPC vesicles in terms of surface morphology, general stability and morphology after addition of ethanol, and lysis tension. This allowed us to develop a feasible experimental approach for the ethanol flow experiments described in the next section.

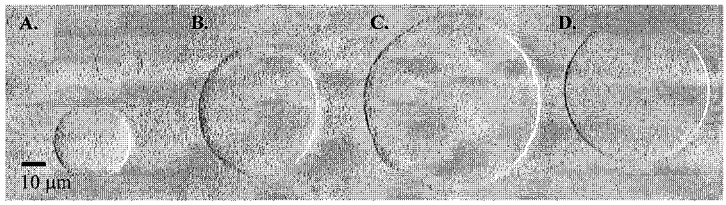

Figure 2 Micrographs of gel phase giant vesicles observed with a 40X Hoffman contrast objective in an isotonic glucose media without alcohol. **(A)** Round DPPC vesicle (bottom) contrasted with an almost transparent ghost DPPC vesicle (top). **(B)** Oblate DPPC vesicle. **(C)** Multifaceted DPPC vesicle. **(D)** Spherically round DPPC/25 mol% Chol vesicle.

DPPC vesicles enclosing 100 mM sucrose in the $L_{\beta'}$ phase were added to an isotonic 100 mM glucose solution without alcohol. We observed a large population of vesicles with a distributed morphology (see figure 2) ranging from completely spherical to multifaceted shapes that most probably depended on the original surface area/volume ratio of the vesicles created during electroformation. We also observed that the percentage of transparent "ghost" vesicles was larger than typically observed in the case of fluid-phase vesicles. When we added the same electroformed DPPC vesicles to an isotonic 100 mM glucose solution containing 10 vol% ethanol (above the $L_{\beta'}$-$L_{\beta}I$ threshold concentration of ~7 vol%), we noticed vesicles displaying the same range of morphology, but a greater number of multifaceted vesicles were seen, presumably due to the induction of the interdigitated state. With or without ethanol, the surfaces of the vesicles appeared rigid and did not thermally fluctuate at room temperature (as expected for the rigid $L_{\beta'}$ and $L_{\beta}I$ phases). These morphological observations agree well with descriptions of gel phase giant vesicles composed of dimyristoyl phosphatidylcholine (DMPC, diC14:0 PC), a shorter chain analog of DPPC.[27,29]

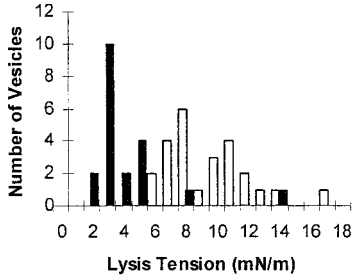

Figure 3 A histogram of the lysis tension values of pure DPPC vesicles mechanically pressurized at a slow pulling rate of 0.1 mN/m/s (black, n=20 vesicles) and high pulling rate of 0.5 mN/m/s (white, n=25 vesicles).

When we aspirated DPPC vesicles at an initial tension of ~1-2 mN/m in an isotonic 100 mM glucose solution without ethanol until membrane failure, the projection length grew monitonically with applied tension, we presume primarily due to the smoothing out of shape deformation. Afterward, the vesicles typically crumpled like "paper sacks" before completely being drawn inside the micropipette within 1-2 seconds. Gel phase lipids are predicted to have higher lysis tension than fluid phase lipids because of their close packing and strong Van der Waals interactions.[27] However, as shown in figure 3 and 10, we found that these vesicles have lysis tension ranging from 1 to 16 mN/m with the majority of aspirated vesicle rupturing around 4 mN/m at a pulling rate of 0.1 mN/m/s. This value can be compared to a recent measured lysis tension value of 9-10 mN/m for fluid phase PC vesicles measured at the same pulling rate of 0.1 mN/m/s.[30] The lower lysis tension value for gel phase DPPC vesicles implies that the vesicles were riddled with surface defects that served as sources for pore nucleation. Stochastic formation of pores, which represents a balance between membrane tension τ and line tension λ, is believed to cause membrane failure if they reach an energetically unstable size.[31] When DPPC vesicles were cooled through the main fluid-gel phase-transition temperature after electroformation, permanent surface defects such as disclinations, holes, or grain-boundaries could form. It is likely that the edges in multifaceted vesicles were grain-boundaries and that ghost vesicles resulted from exchange of solute through surface defects.

Attempts to reduce surface defects by annealing were unsuccessful. Specifically, following the protocols of Kim,[32] we annealed freshly formed gel-phase DPPC vesicles by cycling three times between room temperature and 34 °C (around the ripple-phase transition temperature of 35 °C, but away from the main transition temperature of 41 °C[25]). However, when subjected to micropipette aspiration at a pulling rate of 0.1 mN/m/s, these vesicles continued to rupture around 4-5 mN/m. Perhaps the annealing conditions were insufficient to reduce significantly the surface defect density or that a permanent number of defects always existed in the constrained round or multifaceted vesicles. Therefore, we did not bother to anneal DPPC vesicles used in subsequent MPA experiments. Although the pulling rate of 0.1 mN/m resulted in DPPC vesicles lysing around 4 mN/m, we observed DPPC vesicles lysed at higher tensions (~9 mN/m) as expected when the pulling rate was increased to 0.5 mN/m/s (figure 3 and 10) because measured lysis tension increases with increasing pulling rate.[33,34]

Ethanol Induced Membrane Area Expansion and Threshold Concentration

We monitored projection length growth of DPPC vesicles held by micropipette suction as the vesicles were exposed to flows of isotonic alcohol/water mixtures. Steps were taken in order to assure that the projection growth was entirely due to a phase transition and not to shape-induced deformations under mechanical tension.[27] First, DPPC vesicles enclosing 100 mM sucrose were added to an 85 mM glucose media to inflate them into quasi-spheres without rupturing them. Next, upon aspiration, these vesicles were prestretched beyond 7 mN/m over a very short period of time, 1-2 seconds. Each vesicle's projection length grew inside the micropipette and the outside contour of the vesicle became smoother. The vesicles often still appeared oblate, but further pressurization to increase sphericity (and remove all shape deformations) only resulted in rupture (due to their inherently low lysis tension). The pressure was then relaxed to ≤ or ~2 mN/m wherein the projection length did not decrease and the general shape of the vesicle did not change (as monitored for at least 15 minutes.)

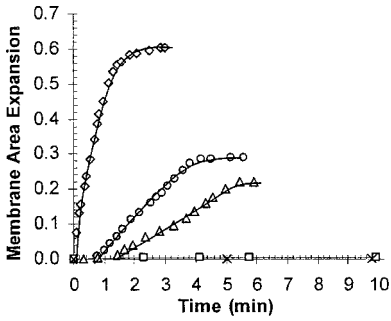

Figure 4 Instantaneous membrane area expansion $(\Delta A/A_{0\%})_{exp}$ of individual vesicles exposed to a flow pipette delivering a constant isotonic ethanol/water mixture stream at specific ethanol concentration (vol): 0% (—×—), 5% (—□—), 8% (—△—), 10% (—○—), and 15% (—◇—). The plateau values of the membrane expansion are reported in figure 5 as equilibrium expansion of the $L_{\beta'}$-$L_{\beta}I$ phase transition. Line fitting is intended as a guide for the eye.

We exposed aspirated DPPC vesicles to a series of ethanol/water mixtures containing 85 mM glucose: 0, 5, 6, 7, 8, 10, 15, and 20 vol% ethanol. The equivalent molar concentrations are 0, 0.85, 1.02, 1.19, 1.36, 1.70, 2.56, and 3.41 M, respectively. For vesicles held at a low tension of ≤1 mN/m and exposed to these isotonic ethanol/water mixtures above 7 vol%, we observed that the oblate shape of the vesicles became wrinkly and folds or creases formed along the surface (presumably from the $L_{\beta'}$-$L_{\beta}I$ phase transition) while the projection length remained unchanged. The low tension of ≤1 mN/m was not sufficient on the timescale of the experiment to pull the excess surface area into the micropipette presumably because of the viscous nature of the interdigitated phase. When the holding tension was larger, ~2 mN/m, we observed that the projection length quickly grew upon exposure to ethanol concentration above 7 vol% as the excess surface area was smoothed out, and the portion of the vesicle external of the pipette maintained its smooth surface. However, at this holding tension, the vesicles were more prone to collapse before the projections reached stable plateaus (possibly due to the fact that thinner membranes have inherently lower lysis tensions[35]). Only runs where stable projections were reached (for example see figure 4) were used for reporting equilibrium $(\Delta A/A_{0\%})_{exp}$. Calculated equilibrium $(\Delta A/A_{0\%})_{exp}$ values from the growth in the projection length and the decrease in the radius of the outer portion of the aspirated vesicle were due to areal

expansion and not due to internal volume change of the vesicle (as discussed in the Material and Methods section). For the equilibrium runs, the projections reached stable plateaus within 3-6 minutes and generally remained unchanged until spontaneous rupture occurred or the flow was manually removed. In the presence of an isotonic glucose solution flow (no ethanol), we observed practically no change in $(\Delta A/A_{0\%})_{exp}$ as shown in figure 4.

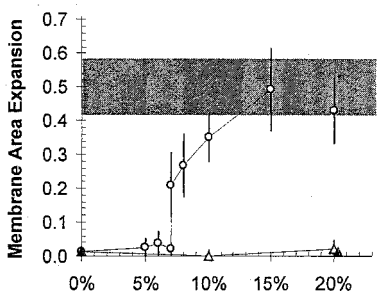

Figure 5 Equilibrium membrane area expansion $(\Delta A/A_{0\%})_{exp}$ vs. ethanol concentration for vesicles with 0 mol% Chol (—○—), 10 mol% Chol (—△—), and 25 mol% Chol (▲). The shaded region represents the expected membrane area when the complete surface fully interdigitates. For 0 mol% Chol at 0%, 5%, 6%, 7% bottom, 7% top, 8%, 10%, 15%, and 20% ethanol (vol), n = 8, 6, 13, 5, 5, 7, 9, 6, and 9, respectively where n is the number of vesicles averaged. For 10 mol% Chol at 10% and 20% ethanol (vol), n = 4 and 6 while for 25% Chol at 20% ethanol (vol), n = 4. Bar indicates one standard deviation.

Equilibrium $(\Delta A/A_{0\%})_{exp}$ values of vesicles with stable projection lengths are reported in figure 5. We observed a sharp threshold occurring at 7 vol% ethanol. At 6 vol%, no area expansion was observed; above 7 vol%, $(\Delta A/A_{0\%})_{exp}$ increased monotonically from 20% to 50% with increasing ethanol concentration. The area expansion at 7 vol% ethanol was bimodal with some vesicles displaying no change in membrane area while others expanded around 20%, and the bimodal distribution appeared invariant with holding tension ranging from 1 to 2 mN/m. This threshold ethanol concentration of 7 vol% for induction of area expansion of giant unilamellar DPPC vesicles concurs with previously reported values of 6.3 vol% for induction of the $L_{\beta'}$-L_{β}I transition as measured by DSC of multilamellar vesicles.[36] Measurement by X-ray diffraction of multilamellar DPPC vesicles revealed that upon full interdigitation, the membrane thickness of 4-5 nm

decreased by 1.6 nm.[1] Similarly, AFM studies on single supported DPPC bilayer showed that the membrane thickness of 5.7 nm decreased by 1.9 nm[37] when interdigitation occurred. For this membrane decrease of ~33 ± 4%, we would expect that when the membrane lipid fully interdigitates, the membrane area should expand around 50 ± 8% (with the assumption that the volume of the hydrocarbon core of the lipid membrane is generally conserved as measured by wide angle reflection of DPPC multibilayers in a large range of ethanol/water mixtures[6]). Though we clearly see a sharp difference in area expansion beyond 7 vol% ethanol, a strong indication that interdigitation occurred, the values between 7 and 15 vol% are below the predicted value of 50% for full interdigitation. There are two possible rationales. The complete membrane of the giant aspirated vesicle became partially interdigitated. This seems thermodynamically implausible. The incomplete packing of the rigid lipid chains would signify a considerable loss of van der Waals interaction energy, and the voids created between the lipid hydrocarbon tails for exposure to water would be highly energetically unfavorable. The more probable rationale is that instead of the entire membrane being fully interdigitated, only large regions or domains of DPPC lipids in the membrane were fully interdigitated while the rest of the membrane remained in the noninterdigitated state. This view is consistent with AFM studies that showed noninterdigitated and interdigitated DPPC domains coexisted on the mica surface in the presence of ethanol below 20 vol% ethanol.[37] At 20 vol% ethanol, the area fraction of the interdigitated phase was 100%. Vierl et al.[6] drew a phase diagram of DPPC in various water-ethanol mixtures (based on the combination of calorimetric, fluorescence, dynamic light scattering, and X-ray diffraction data) that showed both the noninterdigitated and interdigitated phases can coexist for ethanol concentration higher than ~7 vol% in a temperature range of 18 and 25 °C. Other supporting evidence for the coexistence of the fully interdigitated and non-interdigitated phases are found in fluorescent studies of multilamellar DPPC vesicles in the presence of ethanol,[12] X-ray diffraction of dihexadecylphosphatidylcholine (DHPC)/cholesterol vesicles,[13] and high-pressure light transmission of DPPC multilamellar vesicles in the presence of the anesthetic tetracaine.[38] Consequently, figure 5 shows that the size of the fully interdigitated region grew proportionally with increasing ethanol concentration from 7 to 15 vol%. At 7 vol%, about half of the membrane was interdigitated, and at 15 vol%, the whole membrane became interdigitated.

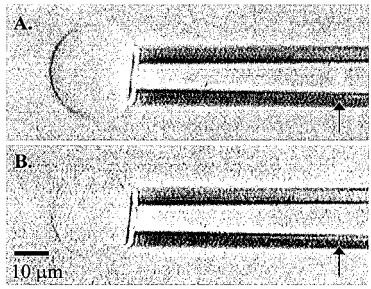

Figure 6 Images of an aspirated DPPC vesicle after being exposed to a flowing stream of an isotonic glucose solution containing 10 vol% ethanol for 7 minutes. **(A)** The projection has reached a stable plateau after undergoing the $L_{\beta'}$-$L_{\beta}I$ phase transition with a $(\Delta A/A_{0\%})_{exp}$ value of 30% with no detectable internal volume loss in the vesicle within experimental error. **(B)** After the flow pipette was removed, the projection length remained unchanged for over 35 minutes, indicating a kinetically trapped interdigitated state. Reducing the holding tension from 2 to 0.2 mN/m caused the surface of the vesicle outside the pipette to wrinkle. Arrows indicate the edge of the projection length.

Kinetically Trapped Ethanol Membrane Area Expansion

When the projection growth reached a plateau during exposure to an isotonic ethanol/water mixture, the plateau generally remained stable for a very short time (< 1 minute). On few occasions, some plateaus were stable for a longer period (3 to 5 minutes). For these vesicles, we moved the flow pipette away from the vesicle and stopped the flow. We expected the projection length to slowly retract as ethanol molecules in the vesicle's interior, in the membrane, and outside media diffused away and caused the interdigitated membrane to undergo a phase transition back to the gel $L_{\beta'}$ phase. This expectation was based upon our previous work with fluid phase PCs in which we demonstrated, by the same MPA-flow technique, that the area expansion caused by exposure to short-chain alcohols was reversible.[14] Instead, we observed that for interdigitated DPPC vesicles with 10 vol% ethanol/water media removed, the projection length remained unchanged (see figure 6). Reducing the holding tension from ~2 mN/m to ~0.2 mN/m should induce the projection length to withdraw; instead only the surface of the DPPC vesicle outside the micropipette relaxed to its corrugated shape (figure 6B). Apparently, the DPPC vesicle was kinetically trapped in the interdigitated state though certainly the ethanol concentration in the surrounding aqueous media was nearly zero as sufficient time (minutes) had passed for the small amount of added ethanol to disperse into the chamber. This ostensibly irreversible effect had been previously observed using DSC that showed

the $L_{\beta}I$-$L_{\beta'}$ phase transition for PCs can be very slow, requiring weeks to reach completion.[5] AFM studies showed the supported interdigitated domains remained stable for a period of days after the ethanol was removed from the bathing solution.[37] However, heating the interdigitated domains above the main phase transition restored the noninterdigitated bilayer. Interestingly, this effect of an irreversible phase transition is being applied to construct a multicompartmental aggregate of tethered vesicles encapsulated within a large bilayer vesicle, known as a vesosome.[11]

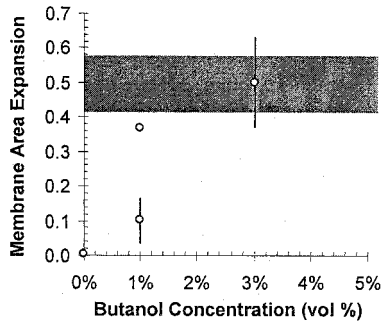

Figure 7 Equilibrium membrane area expansion $(\Delta A/A_{0\%})_{exp}$ vs. butanol concentration. The shaded region represents the expected membrane area when the complete surface fully interdigitates. For 1% (bottom), n=5; 1% (top) n=2; and 3% n=6 where n is the number of vesicle averaged. Bar indicates one standard deviation except at 1% where both values are equal to 0.37.

Butanol Membrane Expansion, Threshold Concentration, and Traube's Rule

Alcohols of longer chain length than ethanol have been shown to induce the interdigitated state in DPPC membranes at much lower concentrations.[39] Indeed, our MPA-flow experiments confirmed that giant DPPC vesicles exposed to an isotonic 1 vol% butanol/water solution was sufficient to induce the interdigitated state as shown in figure 7. A bimodal distribution was observed at 1 vol% butanol where some vesicles showed $(\Delta A/A_{0\%})_{exp}$ value of ~10% while others exhibited ~35%. A higher butanol concentration of 3 vol% caused all vesicles to expand around 50%, signifying that the surfaces were completely interdigitated. The observation of interdigitation at 1 vol% butanol for giant unilamellar vesicles agrees favorably with previously reported values of 1.2 vol% for the

threshold concentration necessary for interdigitation measured by titration calorimetry and DSC of multilamellar vesicles.[40]

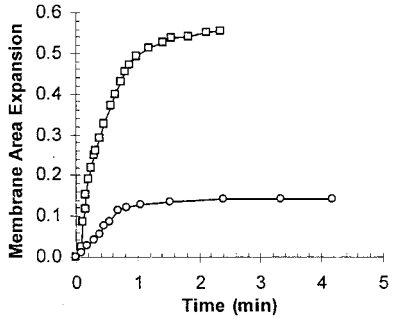

Figure 8 Instantaneous membrane area expansion $(\Delta A/A_{0\%})_{exp}$ of individual vesicles exposed to a flow delivering a butanol/water mixture at 1 vol% (—o—) and 3 vol% (—□—).

A comparison of figure 8 to figure 4 shows the timescale for $L_{\beta'}$-$L_{\beta}I$ phase transition was considerably shorter for vesicles exposed to butanol than ethanol near their respective threshold concentrations. Projection lengths of vesicles exposed to ethanol equilibrate within 3-4 minutes while vesicles exposed to butanol quickly equilibrated within 1 minute. Presumably, butanol's enhanced hydrophobicity from its longer hydrocarbon tail led to enhanced partitioning of the alcohol molecules into the DPPC membrane.[14,40]

Previously reported threshold concentrations for the short-chain alcohol family (methanol, ethanol, propanol, and butanol) in molarity units were 2.5, 1.02, 0.33, and 0.13 M (or in volumetric units are 10.1, 6.3, 2.5, and 1.2 vol%).[39,40] Note that the difference between each number is approximately a factor of three, signifying that for each additional alcohol CH_2 group, the concentration required to induce the $L_{\beta'}$-$L_{\beta}I$ phase transition was reduced roughly by a factor of three. This finding follows Traube's rule of interfacial tension reduction of a hydrophobic-water/alcohol interface due to alcohol adsorption at the interface, i.e. for each additional CH_2 group, the concentration required to reach the same interfacial tension was reduced by a factor of three.[41] As we discussed in our previous work on the adsorption of short-chain alcohols into fluid phase 1-stearoyl, 2-oleoyl phosphatidylcholine (SOPC) membrane, enhanced partitioning of alcohol molecules into the membrane with increasing chain length is at the root of the Traube's rule effect.[14]

Hence, it is likely that the $L_{\beta'}$-$L_{\beta}I$ phase transition is triggered when the surface alcohol concentration in the $L_{\beta'}$ state reaches a single critical value as noted by other investigators,[42,43] and the bulk alcohol concentration required to reach that value decreases by a factor of three for each additional CH_2 group. Mole fractions or partition coefficients of alcohol adsorption in the $L_{\beta'}$ state are difficult to measure and unavailable,[40] but Rowe (1985) showed the critical amount in the fluid phase DPPC was ~0.10 mole fraction to induce the L_{α}-$L_{\beta}I$ phase transition for methanol, ethanol, and propanol.

Impact of Cholesterol on Ethanol Induced Membrane Area Expansion

The incorporation of cholesterol into the gel phase DPPC membrane is known to inhibit the induction of the $L_{\beta'}$-$L_{\beta}I$ phase transition above the alcohol threshold concentration.[12,44] To further investigate this phenomenon, we formed giant vesicles containing DPPC and 10 mol% or 25 mol% Chol for use in MPA-flow studies similar to those performed using pure DPPC vesicles. These vesicles appeared spherically round (figure 2D). No multifaceted vesicles were observed, and at various times, the membrane surface thermally undulated showing that surface rigidity was removed. Upon aspiration into a micropipette, the contour of the vesicle outside the pipette always appeared completely round. The vesicle's projection inside the pipette increased linearly with increasing suction pressure, and the process showed a perfectly reversible (elastic) recovery upon decreasing membrane tension (see figure 9). According to the DPPC:Chol phase diagram, DPPC and 10 mol% Chol should exist in between the gel phase and gel – liquid-ordered phase coexistence regime at room temperature. The DPPC and 25 mol% Chol bilayer exists only in the liquid-ordered phase which exhibits simultaneously fluid and solid like properties.[45] Our observations are consistent with the presence of a liquid-ordered phase in which free moving lipids and cholesterol eliminates any long-lived surface defects and surface rigidity.[46]

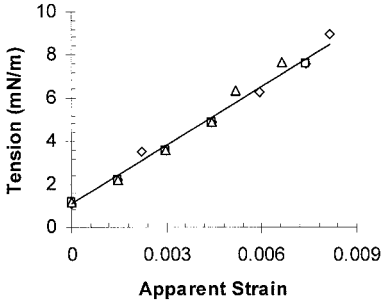

Figure 9 Tension-strain plot of DPPC/10 mol% Chol showing its reversibility when tension was increased (◇) to a high value, decreased (□) back to its initial holding tension, and increased until the vesicle ruptured (△) at a pulling rate of 0.2 mN/m/s. The K_{app} value is 930 mN/m.

DPPC/Chol vesicles aspirated with a holding tension of ~2 mN/m in a 100 mM glucose solution were exposed to an isotonic ethanol/water flow stream with specific ethanol volume concentration of either 0%, 10% or 20%. We observed no increase in the projection length, indicating that induction of the $L_{\beta'}$-$L_{\beta}I$ phase transition was inhibited in vesicles containing 10 mol% or 25 mol% cholesterol (see figure 5). Komatsu and Rowe (1991)[12] showed with flurophores covalently coupled to the ends of the DPPC acyl chains that the induction was completely prevented by the presence of 20 mol% Chol in 12 vol% ethanol. Therefore, our experiment shows that an even lower concentration (10 mol%) will abolish the transition in DPPC/Chol bilayers. Our value is consistent with Lu et al.[47] who showed that at 25 °C, 10 mol% Chol incorporated in 30 mol% 16:0 lysophosphatidylcholine (LPC) / DPPC vesicles inhibits the $L_{\beta'}$-$L_{\beta}I$ phase transition that would otherwise had been induced by the 30 mol% presence of LPC. DSC measurements revealed that the noninterdigitated bilayer structure of 30 mol% LPC / DPPC with 10 mol% Chol incorporation was more thermodynamically stable than the interdigitated phase of 30 mol% LPC / DPPC as evidenced by the bilayer having a significant lower main phase transition temperature ($L_{\beta}I$ - L_{α}) and phase transition enthalpy. A lower amount of 5 mol% Chol has been reported to eliminate completely the interdigitated phase for the DHPC gel phase systems.[13]

The Influence of Ethanol on Mechanical Properties of DPPC/Cholesterol Vesicles

Unlike DPPC vesicles, vesicles formed of DPPC/Cholesterol did not lyse at low tensions and had smooth membrane contours. Therefore, using micropipette aspiration, we could obtain sufficient tension, τ, vs. areal strain, α, data to determine the influence of ethanol on area compressibility, K_{app}, and lysis tension, τ_{lys}, of DPPC/Chol bilayers. DPPC/Chol vesicles containing 10 mol% or 25 mol% Chol formed in 100 mM sucrose were placed in an isotonic 100 mM glucose solution containing 0%, 10%, or 20% ethanol (vol). Subsequent micropipette aspiration resulted in reversible linear growth in the projection length as the suction pressure was increased (figure 9). Following common micropipette convention,[28] the slope of this line is the apparent area compressibility moduli K_{app}, and average values are listed in table 1.

Table 1. Area compressibility moduli K_{app} (mN/m) obtained for giant unilamellar vesicles by the micropipette aspiration method

Cholesterol content in DPPC/Cholesterol Vesicle (mol%)	Ethanol Concentration (vol%)		
	0	10	20
10	900 ± 240 (10)	810 ± 160 (9)	760 ± 290 (4)
25	1200 ± 220 (9)	-	750 ± 90 (11)

*Parentheses represented number of vesicles measured. The difference between the K_{app} values of vesicles with 10 mol% and 25 mol% Chol in 0 vol% ethanol is P=0.013 (as evaluated by Student's t-test) whereas the difference between the K_{app} values of vesicles with 25 mol% Chol in 0 and 20 vol% ethanol is P= 0.0002.

The K_{app} values of DPPC vesicles with 10 and 25 mol% cholesterol content of 900 ± 240 and 1200 ± 220 mM/m, respectively, are higher but within order of the value of 740 ± 100 mN/m reported for DPPC vesicles with 40 mol% cholesterol.[48] Direct measurement of K_{app} values for DPPC bilayer membrane with or without cholesterol appeared to be limited in the literature although the K_{app} value for the shorter-chain analog DMPC exists as well as K_{app} values for fluid-phase SOPC bilayer with cholesterol.[26,27,49] Evans and Needham[27] listed the K_{app} value for the pure gel-phase DMPC as 860 ± 140 mN/m. This predicted value's similarity to our measured K_{app} values with the addition of either 10 or 25 mol% cholesterol is consistent with current knowledge that cholesterol, when added to the membrane, has the unusual property of maintaining strong membrane cohesion while simultaneously softening the membrane by abolishing surface rigidity.[49] For example,

for fluid-phase SOPC vesicles, inclusion of 50 mol% cholesterol had been shown to quadruple the K_{app} value from 200 to 800 mN/m.[49,50]

When we pressurized DPPC/Chol vesicles to measure their K_{app} values in a 10% or 20% (vol) ethanol/water mixture, the DPPC/Chol vesicles behaved elastically, similar to their counterparts in an ethanol-free/water mixture. However, DPPC/10 mol% Chol in 20 vol% ethanol behaved elastically only below 8.3 ± 1.4 mN/m and yielded plastically above this value (discussed in next section). As shown in table 1, the average K_{app} values for DPPC/10 mol% Chol of 810 ± 160 mN/m in 10 vol% ethanol and 760 ± 290 mN/m in 20 vol% ethanol (in the elastic regime) are comparable to 900 ± 240 mN/m in 0 vol% ethanol. However, the average K_{app} value for DPPC/25 mol% Chol of 750 ± 90 mN/m in 20 vol% ethanol is significantly lower than 1200 ± 220 in 0 vol% ethanol. Apparently, the ethanol's interactions with DPPC/25 mol% Chol membrane partially decreased the membrane cohesion, and this implies that perhaps adsorption of ethanol molecule at the bilayer-water interface has reduce the surface energy per monolayer of the membrane. The difference in the K_{app} values further suggests that during the MPA-flow experiments, we might observe a small $(\Delta A/A_{0\%})_{exp}$ value from mechanical deformation as the K_{app} decreases from ethanol exposure. The following calculation will show that $(\Delta A/A_{0\%})_{exp}$ would be too minuscule to notice. The expected area strain $\alpha(K_{app})$ can be estimated with this equation:

$$\alpha(K_{app}) = \tau\left(\frac{1}{K_{app,\,alcohol}} - \frac{1}{K_{app,\,water}}\right) \tag{3}$$

where τ is the holding tension set at 2 mN/m, $K_{app,\,alcohol}$ is the average area compressibility modulus of vesicles in a specific alcohol/water mixture, $K_{app,\,water}$ is the average area compressibility modulus of vesicles in an aqueous mixture without alcohol. The $\alpha(K_{app})$ computed is less than 0.0009, and indeed no area expansion was seen, as evidenced in figure 5.

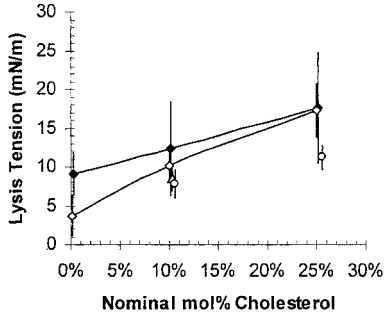

Figure 10 Lysis tension τ_{lys} of DPPC/Chol vesicles suspended in various ethanol concentration (vol %) and subjected to different pulling rates: 0 vol % ethanol, 0.5-0.7 mN/m/s (—♦—); 0 vol %, 0.1-0.2 mN/m/s (—◇—); 10 vol%, 0.2 mN/m/s (△); and 20 vol %, 0.2 mN/m/s (○). The average values are based on 10-20 vesicles. Bar indicates one standard deviation.

In a separate set of experiments, we performed micropipette aspiration in order to determine the lysis tension values of DPPC vesicles containing 10% or 25% (mol) cholesterol in 0%, 10%, or 20% (vol) ethanol (figure 10). For vesicles in 0% ethanol subjected to a pulling rate of 0.5-0.7 mN/m/s, inclusion of 10 and 25 mol% Chol increased the average lysis tension value from 9 ± 3 mN/m at 0% Chol to 13 ± 6 and 18 ± 7 mN/m, respectively. At the medium pulling rate between 0.1 to 0.2 mN/m/s, 10 and 25 mol% Chol substantially raised the lysis tension value from 4 ± 3 mN/m at 0% Chol to 10 ± 2 and 17 ± 3 mN/m, respectively. Surprisingly, the lysis tension values at both 10 and 25 mol% cholesterol showed no strong dependence on pulling rates from 0.1 to 0.7 mN/m/s. Extrapolation of the lines in figure 10 to 40% cholesterol results in an average lysis tension value of approximately 24 mN/m which compared favorably with reported value of 23 ± 3 for DPPC/40 mol% Chol.[48] Cholesterol toughened the surface of the DPPC/Chol vesicles by plausibly ameliorating surface defects and maintaining high membrane cohesion.

Figure 10 shows the lysis tensions of DPPC vesicles with 25 mol% Chol in 20 vol% ethanol were significantly reduced compared to systems without ethanol, while the lysis tensions of DPPC/10 mol% Chol were slightly reduced. This trend is in good agreement with the trend in K_{app} values of DPPC/Chol vesicles as shown in table 1. This is to be expected since the K_{app} value is linearly related to the lysis tension assuming a constant

value for the areal strain at rupture. The areal strains at rupture for DPPC vesicles with 10 and 25 mol% Chol are 0.009 ± 0.004 and 0.012 ± 0.004, respectively, and remain unchanged in the presence of ethanol.

Cholesterol and Pressure-Induced Interdigitation

Above a yield tension of 8.3 ± 1.4 mN/m (n=4 vesicles, close to its lysis tension of 7.9 ± 1.8 mN/m), we observed that DPPC/10 mol% Chol vesicles in 20 vol% ethanol yielded plastically over minutes before the membrane collapsed within 1 to 2 seconds (see figure 11A). To ensure that the large growth in the projection was not simply due to lysis of the vesicle (where the vesicle would vanish away within 1-2 seconds) or volume change from pore formation, we held each pressure increment for ~1 minute (see figure 11B). No stable plateaus of the plastic deformation were ever seen, but the measured membrane area growth that occurred over minutes before collapsed varied from 7% to 20%. This showed that although 10 mol% Chol inhibited the induction of the $L_{\beta'}$-$L_{\beta}I$ phase transition in 20 vol% ethanol, the effect was negated when the mechanical tension (from an applied suction pressure) exceeded a critical value. We then verified this finding by performing MPA-flow experiments. As shown in figure 5, no membrane expansion occurred when DPPC/10 mol% Chol vesicles, held at a tension of 2 mN/m, were exposed to 20 vol% ethanol for a long period of time (over 8-10 minutes). However, when the holding tension was increased to ~9 mN/m, on a few occasions, we observed a large $(\Delta A/A_{0\%})_{exp}$ value, on average of 10%, before the vesicle disappeared (data not shown).

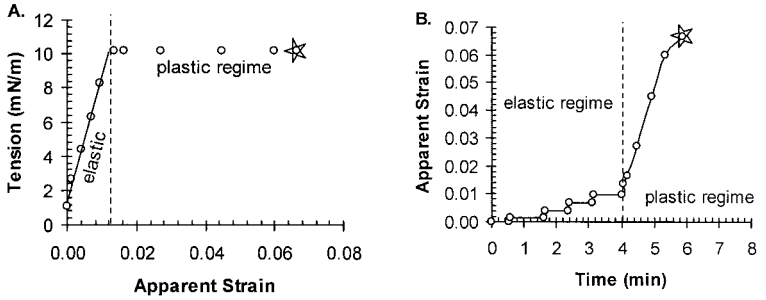

Figure 11 Tension-strain plot of a DPPC/10 mol% Chol vesicle in 20 vol% ethanol. At the yield tension of 10.2 mN/m, the $L_{\beta'}$-$L_{\beta}I$ phase transition was induced. **(A)** From the slope of the line up to the yield tension, K_{app} is 720 mN/m. **(B)** The strain rate is 0.003 min^{-1} at a pulling rate of 0.04 mN/m/s for the first 4 minutes where a holding time of ~1 minute followed each pressure increment. The star symbol represents the point at which the vesicle collapsed.

High pressure-induced interdigitation of saturated PCs in aqueous solutions are well documented in literature out of interest in understanding pressure-anesthetic antagonism, the adaptation of marine organisms to extreme depths, and the sterilization in food processing by high pressure.[3,51-53] Yet, this is the first reporting of low pressure-induced interdigitation of membranes. A high hydrostatic pressure P of ≥70 MPa was generally necessary to induce the $L_{\beta'}$-$L_{\beta}I$ phase transition in DPPC membranes.[54] The yield tension of 8.3 ± 1.4 mN/m for our DPPC/10 mol% Chol system in 20 vol% ethanol is equivalent to a low hydrostatic pressure of 4 MPa based on the formula $P=\tau/H$.[55] H is the effective size of the lipid molecule in the normal direction to the lamella surface: $H^{\beta}=2l\cos\theta$ in the $L_{\beta'}$ state, $H^{in} \approx l$ in the $L_{\beta}I$ state where l is the length of the lipid chain $l = n \times 1.27 \times 10^{-10}$ m; n is the number of carbon groups; θ is the chain tilt in the $L_{\beta'}$ state. A recent theoretical model based on membrane mechanical properties and consistent with experimental results has been proposed by Levadny et al.[55] for PCs in an aqueous solution without alcohol in a high hydrostatic pressure environment (>70 MPa). They discussed that the induced mechanical tension from the applied pressure in the lipid heads region is considerably relieved by a phase transition from either the L_{α} or $L_{\beta'}$ to the interdigitated $L_{\beta}I$ phase. Our observation of a much lower pressure of 4 MPa for our DPPC/10 mol% Chol system in 20 vol% ethanol is most likely due to the presence of a high concentration of ethanol. Ethanol and pressure can work cooperatively to induce interdigitation, as described by Zeng and Chong.[56]

Conclusions

In this work, we applied micropipette aspiration to giant DPPC unilamellar vesicles, thus enabling direct characterization of the areal expansion of the gel ($L_{\beta'}$) phase induced by exposure to short-chain alcohols: ethanol and butanol. Areal expansion began at a threshold ethanol concentration of 7 vol% and increased monotonically with increasing ethanol concentration until 15 vol% at which point the areal expansion reached a plateau of 50%. These observations are consistent with the known physical characteristics of the DPPC interdigitated ($L_{\beta}I$) phase induced by alcohols (as investigated by X-ray diffraction, AFM, and DSC), and hence, our findings are the first direct measurement of the areal expansion that accompanies the $L_{\beta'}$-$L_{\beta}I$ phase transition. For ethanol concentrations between 7 vol% and 15 vol%, areal expansion increased monotonically, consistent with

the existence of domains of the $L_{\beta}I$ and $L_{\beta'}$ phases in coexistence, but for 15 vol% or higher, the observed constant areal expansion indicates that 100% $L_{\beta}I$ phase exists. At the 7 vol% ethanol threshold concentration, the area expansion exhibited a bimodal distribution of 0% and 20%, indicating that at the threshold concentration, interdigitation is induced in only a portion of DPPC vesicles. Areal expansion could not be easily reversed, consistent with kinetic trapping of the $L_{\beta}I$ phase. DPPC vesicles exposed to butanol and ethanol exhibited similar areal expansion behaviors, but the threshold concentration for butanol is much lower, 1 vol%, compared to ethanol suggesting that the threshold concentrations (in molar concentration) for short-chain alcohols follows Traube's rule; that is for every additional CH_2 group, three times less alcohol is needed to induce interdigitation. Ethanol-induced areal expansion of DPPC bilayers was inhibited by inclusion of 10 mol% and 25 mol% cholesterol in the bilayer, consistent with improved stability of a liquid-ordered phase. However, areal expansion of DPPC-cholesterol bilayers could be induced by the simultaneous presence of ethanol and application of tension (~8 mN/m), suggestive of a cooperative effect. The presence of 20 vol% ethanol significantly decreased the surface cohesion of DPPC bilayers containing 25 mol% cholesterol as evidenced by a decreased area compressibility modulus and lysis tension. Lastly, these palpable effects on the mechanical properties and area of a lipid membrane in the gel and liquid-ordered phases induced by short-chain alcohols compliment our previous parallel studies on a fluid phase membrane. Given the broad distribution of membrane components, it is highly likely that gel phase, fluid phase, and liquid ordered phase coexist in eukaryotic cell membranes, including those that contain sterols other than cholesterol. These studies demonstrate that significant (and possibly reversible) changes in area per molecule and values of mechanical properties are to be expected in all lipid phases of cell membranes after exposure to concentrations of short-chain alcohols in which major alterations in the metabolism of organisms, especially eukaryotic micro-organisms, have been observed.

Acknowledgements

We would like to thank Professor David Block of the Departments of Chemical Engineering and Materials Science and Viticulture and Enology at the University of California, Davis, for inspiring us in these studies. This work was funded by the Materials

Research Institute at Lawrence Livermore National Laboratory (MI-03-117), the Center for Polymeric Interfaces and Macromolecular Assemblies (Grant NSF DMR 0213618), and the generous endowment from Joe and Essie Smith.

[1] S. A. Simon; T. J. McIntosh, *Biochim. Biophys. Acta* **1984**, *773*, 169-172.
[2] J. L. Slater; C. H. Huang, *Prog. Lipid Res.* **1988**, *27*, 325-359.
[3] L. F. Braganza; D. L. Worcester, *Biochemistry* **1986**, *25*, 2591-2596.
[4] O. P. Bondar; V. G. Pivovarenko; E. S. Rowe, *Biochimica Et Biophysica Acta-Biomembranes* **1998**, *1369*, 119-130.
[5] E. S. Rowe; T. A. Cutrera, *Biochemistry* **1990**, *29*, 10398-10404.
[6] U. Vierl; L. Lobbecke; N. Nagel; G. Cevc, *Biophys. J.* **1994**, *67*, 1067-1079.
[7] N. E. Nagel; G. Cevc; S. Kirchner, *Biochim. Biophys. Acta* **1992**, *1111*, 263-269.
[8] N. A. Avdulov; S. V. Chochina; L. J. Draski; R. A. Deitrich; W. G. Wood, *Alcoholism-Clinical and Experimental Research* **1995**, *19*, 886-891.
[9] J. L. Slater; C. H. Huang, in: "*The Structure of Biological Membranes*"; P., Y., Ed.; CRC Press: Boca Raton, FL, 1992; pp 175-210.
[10] H. Komatsu; S. Okada, *Biochimica Et Biophysica Acta-Biomembranes* **1995**, *1235*, 270-280.
[11] E. T. Kisak; B. Coldren; J. A. Zasadzinski, *Langmuir* **2002**, *18*, 284-288.
[12] H. Komatsu; E. S. Rowe, *Biochemistry* **1991**, *30*, 2463-2470.
[13] P. Laggner; K. Lohner; R. Koynova; B. Tenchov, *Chem. Phys. Lipids* **1991**, *60*, 153-161.
[14] H. V. Ly; M. L. Longo, *In Revision at Biophysical Journal* **2003**.
[15] D. Needham; D. V. Zhelev, in: "*Giant Vesicles*"; Luisi, P. L.; Walde, P., Eds.; John Wiley & Sons, LTD, 2000; Vol. 6, pp 103-147.
[16] D. Needham; D. V. Zhelev, in: "*Vesicles*"; Rosoff, M., Ed.; Marcel Dekker, Inc., 1996; Vol. 62, pp 373-444.
[17] E. A. Evans, *Methods Enzymol.* **1989**, *173*, 3-35.
[18] R. Kwok; E. Evans, *Biophysical Journal* **1981**, *35*, 637-652.
[19] B. M. Discher; Y. Y. Won; D. S. Ege; J. C. M. Lee; F. S. Bates; D. E. Discher; D. A. Hammer, *Science* **1999**, *284*, 1143-1146.
[20] M. L. Longo; A. J. Waring; D. A. Hammer, *Biophysical Journal* **1997**, *73*, 1430-1439.
[21] M. L. Longo; A. J. Waring; L. M. Gordon; D. A. Hammer, *Langmuir* **1998**, *14*, 2385-2395.
[22] D. V. Zhelev; N. Stoicheva; P. Scherrer; D. Needham, *Biophys. J.* **2001**, *81*, 285-304.
[23] D. Needham; D. V. Zhelev, *Annals of Biomedical Engineering* **1995**, *23*, 287-298.
[24] H. V. Ly; D. E. Block; M. L. Longo, *Langmuir* **2002**, *18*, 8988-8995.
[25] J. Silvius, "*Lipid-Protein Interactions*"; John Wiley & Sons: New York, 1982.
[26] D. Needham; E. Evans, *Biochemistry* **1988**, *27*, 8261-8269.
[27] E. Evans; D. Needham, *J. Phys. Chem.* **1987**, *91*, 4219-4228.
[28] W. Rawicz; K. C. Olbrich; T. McIntosh; D. Needham; E. Evans, *Biophys. J.* **2000**, *79*, 328-339.
[29] M. I. Angelova; R. Mutafchieva; R. Dimova; B. Tenchov, *Colloids Surfaces* **1999**, *149*, 201-205.
[30] K. Olbrich; W. Rawicz; D. Needham; E. Evans, *Biophys. J.* **2000**, *79*, 321-327.
[31] B. Deryagin; Y. Gutop, *Kolloidn. Zh.* **1962**, *24*, 370-374.
[32] D. H. Kim; M. J. Costello; P. B. Duncan; D. Needham, *Langmuir* **2003**, *19*, 8455-8466.
[33] E. Evans; F. Ludwig, *Journal of Physics-Condensed Matter* **2000**, *12*, A315-A320.
[34] E. Evans; V. Heinrich; F. Ludwig; W. Rawicz, *Biophys. J.* **2003**, *85*, 2342-2350.
[35] J. C. M. Lee; H. Bermudez; B. M. Discher; M. A. Sheehan; Y.-Y. Won; F. S. Bates; D. E. Discher, *Biotechnol. Bioeng.* **2001**, *73*, 135-145.
[36] E. S. Rowe, *Biochemistry* **1983**, *22*, 3299-3305.
[37] J. Mou; J. Yang; C. Huang; Z. Shao, *Biochemistry* **1994**, *33*, 9981-9985.
[38] S. Maruyama; T. Hata; H. Matsuki; S. Kaneshina, *Biochimica Et Biophysica Acta-Biomembranes* **1997**, *1325*, 272-280.
[39] E. S. Rowe, *Biochim. Biophys. Acta* **1985**, *813*, 321-330.
[40] F. Zhang; E. S. Rowe, *Biochemistry* **1992**, *31*, 2005-2011.
[41] I. Traube, *Ann. Chem. Liebigs* **1891**, *265*, 27-55.
[42] L. Loebbecke; G. Cevc, *Biochim. Biophys. Acta* **1995**, *1237*, 59-69.
[43] E. S. Rowe; J. M. Campion, *Biophys. J.* **1994**, *67*, 1888-1895.
[44] M. F. N. Rosser; H. M. Lu; P. Dea, *Biophys. Chem.* **1999**, *81*, 33-44.

[45] T. P. W. McMullen; R. N. A. H. Lewis; R. N. Mcelhaney, *Biochemistry* **1993**, *32*, 516-522.
[46] S. L. Veatch; S. L. Keller, *Physical Review Letters* **2002**, *8926*, 8101.
[47] J. Z. Lu; Y. H. Hao; J. W. Chen, *J. Biochem. (Tokyo).* **2001**, *129*, 891-898.
[48] E. Endress; S. Bayerl; K. Prechtel; C. Maier; R. Merkel; T. M. Bayerl, *Langmuir* **2002**, *18*, 3293-3299.
[49] D. Needham; R. Nunn, *Biophys. J.* **1990**, *58*, 997-1009.
[50] E. Evans; W. Rawicz, *Physical Review Letters* **1990**, *64*, 2094-2097.
[51] D. Worcester; B. Hammouda, *Physica B* **1997**, *241*, 1175-1177.
[52] D. A. Driscoll; S. Samarasinghe; S. Adamy; J. Jonas; A. Jonas, *Biochemistry* **1991**, *30*, 3322-3327.
[53] H. Ichimori; T. Hata; H. Matsuki; S. Kaneshina, *Biochimica Et Biophysica Acta-Biomembranes* **1998**, *1414*, 165-174.
[54] H. Ichimori; T. Hata; T. Yoshioka; H. Matsuki; S. Kaneshina, *Chem. Phys. Lipids* **1997**, *89*, 97-105.
[55] V. Levadny; V. M. Aguilella; M. Yamazaki, *Chemical Physics Letters* **2002**, *360*, 515-520.
[56] J. W. Zeng; P. L. G. Chong, *Biochemistry* **1991**, *30*, 9485-9491.